Magnetization steps in $Pb_{1-x}Eu_xSe$: Determination and identification of the dominant antiferromagnetic exchange constant

V. Bindilatti and N. F. Oliveira, Jr.
Instituto de Física, Universidade de São Paulo, Caixa Postale 66.318, 05389-970 São Paulo, São Paulo, Brazil

Y. Shapira, G. H. McCabe, and M. T. Liu
Department of Physics, Tufts University, Medford, Massachusetts 02155

S. Isber, S. Charar, and M. Averous
Groupe d'Etude des Semiconducteurs URA 357, Université Montpellier II, Place Eugene Bataillon, 34095 Montpellier Cedex 5, France

E. J. McNiff, Jr.
Francis Bitter National Magnet Laboratory, Massachusetts Institute of Technology, Cambridge, Massachusetts 02139

Z. Golacki
Institute of Physics, Polish Academy of Sciences, Pl. 02-668 Warsaw, Poland
(Received 25 August 1995)

The magnetization of three $Pb_{1-x}Eu_xSe$ samples, with $x=1.3$,3.0, and 4.1 %, was measured at 30 and 50 mK in magnetic fields H up to 50 kOe, and at 0.6 K in fields up to 180 kOe. For $x=1.3\%$ and with $\mathbf{H}\|[100]$, a magnetization step (MST) due to an energy-level crossing for isolated Eu^{2+} ions was observed at 30 and 50 mK. The magnetic field at this MST, 1.76 ± 0.2 kOe, was close to the predicted value $H_c=1.98$ kOe. At the same low temperatures (30 and 50 mK) but at higher fields, a magnetization ''ramp'' due to pairs was observed in all samples. For $x=3.0$ and 4.1 % this ramp consisted of well-resolved MST's arising from pairs. A ramp due to open triplets was also observed in these two samples. The MST's due to pairs were used to obtain the value $J/k_B=-0.24\pm0.03$ K for the dominant antiferromagnetic exchange constant. Comparisons between the measured magnetization curves at 30 or 50 mK and theoretical simulations indicates that this J is the nearest-neighbor (NN) exchange constant J_1. At 0.62 K the magnetization of each of the three samples rose rapidly with H in fields below several kOe. At higher fields a rounded ramp due to pairs and triplets was present. This ramp ended near 40 kOe, and complete saturation was achieved near 50 kOe. A model which includes only the NN exchange constant J_1 gave a reasonably good account for all the data at 0.62 K. Calculated magnetization curves for pairs, and for open and closed triplets, at various values of $k_BT/|J|$ are presented. The effects of the single-ion and dipole-dipole anisotropies on the MST's due to pairs are also discussed.

I. INTRODUCTION

The Eu chalcogenides (EuO, EuS, EuSe, and EuTe) are probably the most extensively studied group of magnetic semiconductors.[1–4] The lead salts (PbS, PbSe, and PbTe) constitute an important group of IV–VI semiconductors. The compounds in both groups have the rocksalt structure, with an fcc cation lattice. Lead salts in which a small fraction of the Pb cations has been replaced by Eu^{2+} ions are examples of IV–VI diluted magnetic semiconductors (DMS).[5] The Eu^{2+} ion is an S-state ion, with very weak interactions with the lattice. The magnetic behavior of this ion is therefore relatively simple, similar to that of Mn^{2+} (which is also an S-state ion) but unlike those of Co^{2+} or Fe^{2+}.

Accurate values for the exchange constants J_i between the Eu^{2+} ions in IV–VI DMS proved difficult to obtain. It is known, however, that these J_i are considerably smaller than those for Mn ions in II–VI DMS (e.g., $Cd_{1-x}Mn_xTe$).[5,6] In this paper we report on direct measurements of the dominant antiferromagnetic (AF) exchange constant for Eu^{2+} ions in PbSe.

In the past decade the magnetization-step (MST) method has emerged as a leading technique for determining exchange constants, and sometimes also single-ion anisotropy parameters.[7–10] Nearly all MST experiments to date were on Mn^{2+} or Co^{2+} ions in II–VI DMS. In such DMS the dominant exchange constant is relatively large, $|J/k_B|\geqslant 10$ K typically, and is antiferromagnetic. (Spins coupled ferromagnetically do not lead to MST's, but in II-VI DMS all exchange interactions are believed to be AF.) The present study of MST's originating from Eu^{2+} ions in $Pb_{1-x}Eu_xSe$ presented two challenges. First, temperatures $T<0.1$ K were required because even the largest AF exchange constant J is only a fraction of 1 K. Second, after measuring J there still remained the question of the identity of this J: is it the nearest-neighbor (NN) exchange constant J_1 or the next-nearest-neighbor (NNN) exchange constant J_2? In the fcc cation lattice, with a lattice constant a, the NN's are separated by $a/\sqrt{2}$ while the NNN's are separated by a. Because of the smaller separation, one may expect that the largest AF interaction is J_1, as in II–VI DMS. However, it is known[1] that in EuSe the NN exchange constant J_1 is ferromagnetic,

so that the largest AF exchange constant in this material is J_2. At the start of this work it was unclear whether J_1 or J_2 was the dominant AF exchange constant in $Pb_{1-x}Eu_xSe$ with low x.

II. THEORY

Relevant theoretical predictions for various types of MST's are summarized in this section. Much of the discussion is based on a model in which the exchange interactions are well represented by a single AF exchange constant J; all other exchange constants are ignored. This single-J model is similar to the J_1 model in Refs. 7–9 except that (1) it does not presuppose that J is necessarily J_1, and (2) it sometimes also includes anisotropic interactions.

The notion of clusters is very useful when the single-J model is applied to DMS with low x. The Eu ions are viewed as belonging to clusters of different types: singles (isolated ions with no exchange bonds), pairs, open triplets, closed triplets, and clusters with more than 3 spins.[7–9] Each type of cluster gives rise to a series of MST's with unique characteristics.

A. MST due to isolated Eu ions

The behavior of an isolated Eu^{2+} ion in PbSe can be described in terms of an effective spin Hamiltonian for spin $S=7/2$. This Hamiltonian, whose form is given by Abragam and Bleaney,[11] contains three parameters: the g factor, and the anisotropy coefficients b_4 and b_6. Recent EPR measurements[12] gave the values $g=1.982$, $b_4=+0.27$ GHz, and $b_6=-0.0026$ GHz.

The calculated energy levels for an isolated Eu^{2+} ion when the magnetic field **H** is parallel to [100] are shown in Fig. 1(a). At the field H_c there is a level crossing which changes the ground state. This change results in an increase of the magnetic moment of the ground state, because the magnetic moment of a state $|i\rangle$ is equal to $-\partial E_i/\partial H$, where E_i is the energy of the state. If the temperature T is low, the magnetization M is controlled by the ground state, so that the level crossing results in a magnetization step. Figure 1(b) shows the calculated magnetization curves at 10 and 50 mK. The levels which cross correspond roughly to states with $S_z=-5/2$ and $-7/2$, where S_z is the spin projection along **H**. Therefore, the ratio between the magnetizations before and after the MST is roughly 5/7. For $\mathbf{H}\|[100]$ the MST is predicted to occur at $H_c=1.98$ kOe.

As the angle θ between **H** and the [100] axis increases from zero, the energy-level crossing at H_c changes to anticrossing. The MST is then broader, and its center is at a lower field. The dependence of the MST on θ was calculated for **H** in the (001) plane. The downward shift of the field at the MST is 0.06 kOe for $\theta=5°$, and about 0.2 kOe for 10°. At $\theta=15°$ (or 75°) the MST becomes very broad. For $20<\theta<70°$, which includes the [110] direction, there is no distinct MST. Additional calculations for $\mathbf{H}\|[111]$ show that for this direction also there is no distinct MST.

B. Simple model for MST's due to pairs and triplets

The main features of the series of MST's which arise from pairs, from open triplets (OT's), and from closed triplets (CT's), are obtained from a simplified version of the single-J model. In this simple version all anisotropic interactions are ignored.[7–9] The Hamiltonian for an isolated ion then does not contain the terms involving b_4 and b_6. The magnetization of isolated Eu ions (singles) therefore follows the Brillouin function, and it does not exhibit the MST described in the preceding section. However, level crossings for pairs, OT's, and CT's do occur, and they lead to MST's at low temperatures.

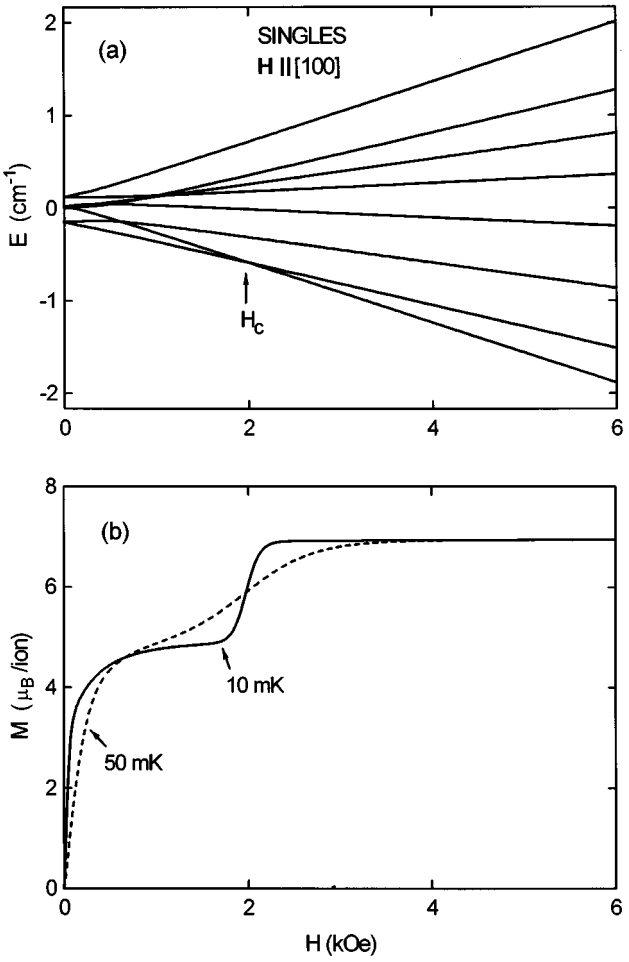

FIG. 1. (a) Energy levels for an isolated Eu^{2+} ion (single) in PbSe as a function of magnetic field H. Note the level crossing at H_c. (b) Calculated magnetization curves for isolated Eu^{2+} ions at 10 and 50 mK. These results are for $\mathbf{H}\|[100]$.

The energy levels for pairs, for OT's and for CT's are known.[13] We used them to calculate the partition function as a function of H. The free energy, and the magnetization M were then obtained numerically. For pairs there also exists an analytic expression for M.[6,14]

1. Magnetization of pairs

The calculated magnetization of pairs at three values of the normalized temperature $\tau\equiv k_BT/|J|$ is shown in Fig. 2(a). Well-resolved MST's occur when τ is low, as illustrated by the curve for $\tau=0.25$. In the present simple model the fields H_n at the centers of the MST's are given by

$$g\mu_BH_n=2|J|n, \tag{1}$$

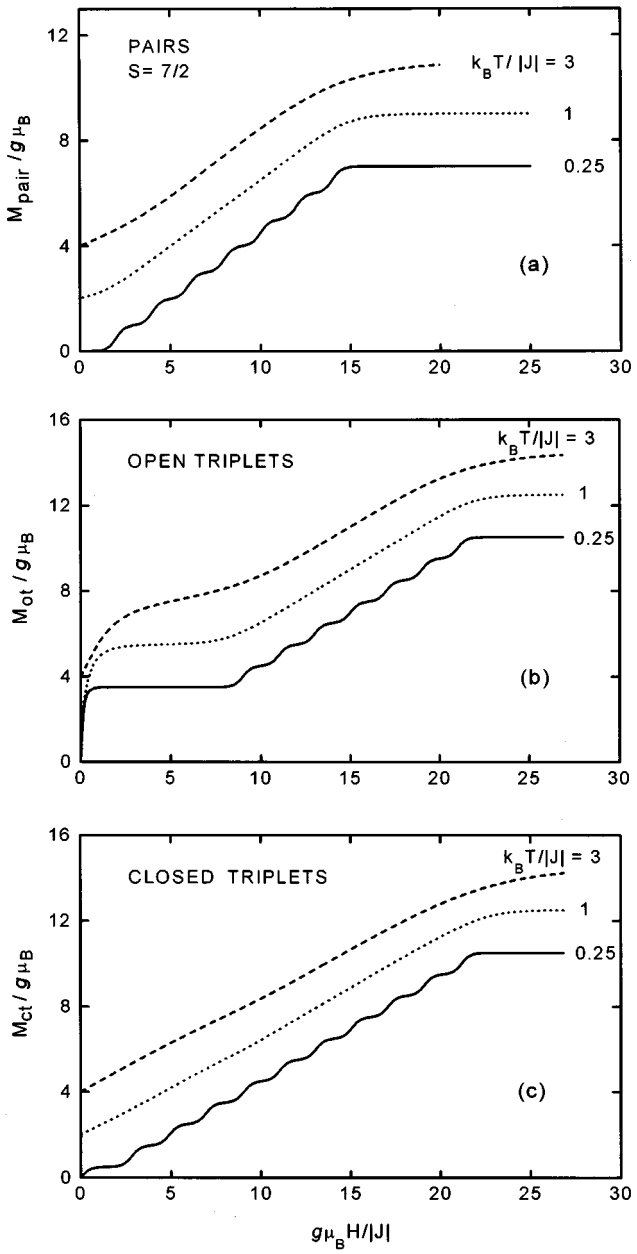

FIG. 2. Calculated magnetization curves for various clusters at three values of the normalized temperature $\tau \equiv k_B T/|J|$. In each case the average magnetic moment per cluster M (in units of $g\mu_B$) is plotted as a function of the normalized magnetic field $g\mu_B H/|J|$. (a) Pairs. (b) Open triplets. (c) Closed triplets. All curves for $\tau=1$ have been moved upward by two units. Curves for $\tau=3$ have been moved upward by four units.

where $n=1,2,\ldots,7$ for Eu^{2+} ($S=7/2$ for each ion). For an arbitrary S, the values of n are $1,2,\ldots,2S$. After the last MST is completed, the pair magnetization saturates at $2Sg\mu_B$.

An estimate of the maximum temperature at which the MST's are resolved is obtained as follows. Each MST corresponds to a peak in dM/dH. The full width at half height, δH, of this peak is given by[9]

$$g\mu_B \delta H = 3.53 k_B T. \tag{2}$$

If one assumes that the MST's are resolved when the separation $\Delta H = H_{n+1} - H_n$ between adjacent MST's exceeds δH, the condition for resolving the MST's is $\tau \equiv k_B T/|J| < 0.6$. Computer calculations of dM/dH indicate that actually the temperature requirement is somewhat less stringent; most of the MST's are still resolved (but only barely) at $\tau=1.0$. These results are true only for the simple model considered now, in which δH is due to thermal broadening only. When other sources of broadening are considered, lower temperatures are required to resolve the MST's.

At normalized temperatures $\tau \cong 1$ the MST's coalesce and form a "ramp," with M increasing approximately linearly with H. The ramp for $\tau=1$ is shown in Fig. 2(a). Increasing τ to 3 results in a rounding of the ramp. Some of our experimental data are in the range where the MST's due to pairs are resolved, but others, at higher temperatures, correspond to rounded ramps. Ramps were observed earlier in other DMS.[15,16]

2. Magnetization of open triplets

The magnetization curves for OT's at three values of τ are shown in Fig. 2(b). Consider first the curve for $\tau=0.25$. At low H there is a rapid alignment of the ground-state magnetic moment. (The ground-state magnetic moment of an OT is equal to 1/3 of its saturation moment, corresponding to a $\uparrow\downarrow\uparrow$ ground-state configuration.) Following the alignment of the ground-state moment, a series of MST's occurs at fields H_r which are given by

$$g\mu_B H_r = r|J|, \tag{3}$$

where $r=9,11,13,\ldots,21$ for Eu^{2+} spins ($S=7/2$). For an arbitrary S the first MST is at $r=2S+2$, and the last at $r=6S$. The spacing of the MST's is the same as that for pairs, but the positions are different. In the present simple model, the criterion $\Delta H > \delta H$ for resolving the MST leads to the same temperature requirement ($\tau<0.6$) as in the case of pairs. As τ increases to 1, the MST's coalesce and form a ramp. The ramp is more rounded at $\tau=3$.

3. Magnetization of closed triplets

Magnetization curves for CT's are shown in Fig. 2(c). The curve at the lowest τ can be understood as follows. For a CT consisting of Eu^{2+} ions the net spin of the ground state is 1/2. The ground-state magnetic moment is therefore equal to 1/21 of the saturation moment of the CT. At $\tau=0.25$ the ground-state moment aligns rapidly with H. Following this alignment, a series of MST's occurs at fields H_k which are given by

$$g\mu_B H_k = k|J|, \tag{4}$$

where $k=3,5,7,\ldots,21$ for $S=7/2$. For an arbitrary half-integer S the first MST is at $k=3$ and the last at $r=6S$. The separation between the MST's is the same as that for pairs, but the positions are different. Once the last MST is completed, the magnetization of the CT's becomes saturated. As in the case of pairs and OT's, the MST's merge into a ramp when $\tau=1$.

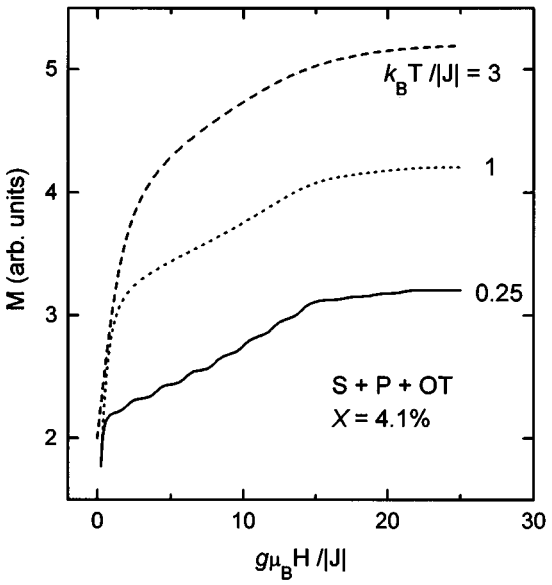

FIG. 3. Theoretical simulations of the magnetization curves for $x=4.1\%$ for three values of $\tau \equiv k_BT/|J|$. The cation lattice is fcc, and J is assumed to be the NN exchange constant J_1. Only singles, pairs, and open triplets are included in the simulations. The curves for $\tau=1$ and 3 have been shifted upward by one and two units, respectively.

4. Simulations of the magnetization curve

The magnetization curve of the sample as a whole is calculated by adding the contributions of singles, pairs, OT's, and CT's. The contribution of larger clusters is neglected. This is an excellent approximation for two of our samples ($x \leqslant 3.0\%$), and is quite a good approximation even for the third sample ($x=4.1\%$). To carry out the calculation it is necessary to know the concentrations of the various clusters. In this work it was always assumed that the distribution of the Eu ions over the cation sites was random. The probabilities of finding various clusters were then obtained from Ref. 17.

For purpose of illustration we take $x=4.1\%$ and assume that J is the NN exchange constant J_1. To simplify the interpretation, we neglect (in this case only) the very small contribution of the CT's. The calculated magnetization curves for $\tau=0.25$, 1, and 3, are shown in Fig. 3. Consider the curve for $\tau=1$. At low fields there is a rapid alignment of the singles and of the ground-state moments of the OT's. This alignment is followed by the ramp due to pairs. A slight increase in slope occurs when the ramp due to OT's begins, near $g\mu_BH/|J|=9$. The ramp due to pairs ends near $g\mu_BH/|J|=14$, but the smaller ramp due to the OT's persists until $g\mu_BH/|J| \cong 21$. Some of these features were previously observed experimentally in $Cd_{1-x}Mn_xTe$ (Ref. 16).

At $\tau=0.25$ the calculated magnetization curve shows MST's due to pairs and OT's. These MST's stand out more clearly in Fig. 4. The derivative dM/dH is also shown in Fig. 4. The MST's appear as peaks in the derivative. One interesting feature is that the peaks from the first few MST's due to the OT's (at $g\mu_BH/|J|=9$, 11, 13) are exactly out of phase with peaks due to pairs. The net effect is that in this field range the peaks due to pairs have a smaller size. The last few small peaks in the derivative ($g\mu_BH/|J|>14$) are due to OT's alone, because by then the magnetization of the pairs is saturated.

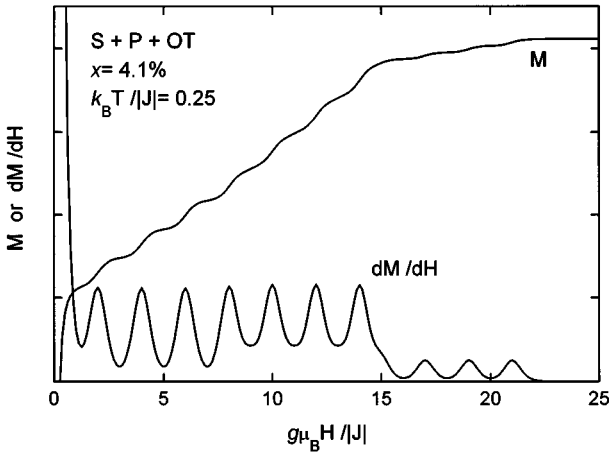

FIG. 4. Expanded view of the top part of the curve for $\tau=0.25$ in Fig. 3. The MST's due to pairs and OT's are clearly visible. Also shown is the derivative dM/dH of this curve.

C. Effects of other interactions on the MST's due to pairs

The simple model in the preceding section considered only the dominant AF exchange constant J. Other exchange constants, $J_i \neq J$, were neglected. All anisotropies were also neglected. The expected effects due to these additional interactions will now be considered.

1. Other exchange interactions

The main effect of the other J_i on the MST's due to pairs is to shift the fields H_n at the MST's. An approximate treatment by Larson *et al.*[18] indicates that Eq. (1) should be replaced by

$$g\mu_BH_n=2|J|n+\Delta_n, \tag{5}$$

where the shift Δ_n is nearly independent of n. Recent numerical results for a simple case[8] suggest that Δ_n is independent of n only when the other J_i are less than $\sim 0.01J$. Typically the other J_i are not so small. Nevertheless, quite accurate values for J are obtained by using Eq. (5) with a constant Δ_n. The reason is that Δ_n is usually an order of magnitude smaller than $2|J|$ and the variation of Δ_n with n is only a fraction of Δ_n.

The other J_i also broaden the MST's because although all pairs are coupled by the same J, the configurations of the other J_i are different for different pairs. Due to the extra broadening, δH is larger than the thermal width given by Eq. (2). As a consequence the temperature requirement for resolving the MST's becomes more stringent.

2. Single-ion anisotropy

In this work J was obtained from the fields H_n of the MST's due to pairs. Two types of anisotropy affect these H_n. First, each spin is subjected to the single-ion anisotropy (cubic anisotropy) involving the parameters b_4 and b_6 in the spin Hamiltonian. Second, there is a dipole-dipole (DD) in-

teraction between the two spins in the pair. The single-ion and DD anisotropies are considered first separately and then together.

The energy levels of a pair in the presence of a single-ion anisotropy were obtained by a numerical diagonalization of the pair Hamiltonian, represented by a 64×64 matrix. The calculations were performed using the relevant parameters for Eu^{2+} in PbSe (b_4 and b_6 as given above, and $J/k_B=-0.24$ K as given below). Results were obtained for **H** parallel to the [100], [110], and [111] directions. The fields where the ground state changes, due to level crossing, gave the values of H_n.

The single-ion anisotropy has a significant effect on H_n. The separation $\Delta H=H_{n+1}-H_n$ between adjacent MST's is no longer independent of n. The largest change of ΔH compared to the value $(\Delta H)_J$ in the absence of anisotropy is for the separation between the sixth and seventh steps (at the highest fields). This particular ΔH is about 40% higher than $(\Delta H)_J$ for $\mathbf{H}\|[100]$, but for **H** parallel to either the [110] or [111] directions this ΔH is about 30% lower than $(\Delta H)_J$. The *average* separation $(\Delta H)_{\rm av}$ between the MST's is much closer to $(\Delta H)_J$. Specifically, $(\Delta H)_{\rm av}$ is 9% higher than $(\Delta H)_J$ for $\mathbf{H}\|[100]$, 4% lower than $(\Delta H)_J$ for $\mathbf{H}\|[110]$, and 7% lower than $(\Delta H)_J$ for the $\mathbf{H}\|[111]$.

In the present work J was obtained from a fit of the measured fields H_2 through H_7 to Eq. (5). The effect of the single-ion anisotropy on the J obtained in this manner was therefore considered. Compared to the true J the exchange constant which is obtained from the fit to Eq. (5) is 9% higher for $\mathbf{H}\|[100]$, 3% lower for $\mathbf{H}\|[110]$, and 6% lower for $\mathbf{H}\|[111]$. For an unknown field direction it is probably safe to assume that the J obtained from a fit to Eq. (5) will be correct to within 10%. Values of Δ_n obtained by fitting the calculated H_2 through H_7 to Eq. (5) were of order 1 kG; negative for $\mathbf{H}\|[100]$ but positive for the other two principal directions.

The results above show that the sign of the change in $(\Delta H)_{\rm av}$ is positive for the [100] direction but negative for the [110] and [111] directions. For some intermediate directions the single-ion anisotropy hardly changes $(\Delta H)_{\rm av}$, e.g., only a 1% change for the [102] direction. The variation of ΔH with n is also much smaller for the [102] direction.

3. Dipole-dipole interaction

The DD energy between two magnetic moments, $\boldsymbol{\mu}_1$, and $\boldsymbol{\mu}_2$, separated by **r** is

$$E_{\rm DD}=(\boldsymbol{\mu}_1\cdot\boldsymbol{\mu}_2/r^3)-3(\boldsymbol{\mu}_1\cdot\mathbf{r})(\boldsymbol{\mu}_2\cdot\mathbf{r})/r^5. \tag{6}$$

The first term is isotropic, similar in form to the isotropic Heisenberg exchange interaction. Its effect is equivalent to a change of J. In the present case the change of the effective J is $+6\%$ if the pair consists of NN spins. The second term in Eq. (6) is anisotropic, i.e., it depends on the direction of the magnetic moments relative to the lattice rather than relative to each other. The shifts in the values of H_n due to this second term were obtained from a numerical diagonalization of the pair Hamiltonian. Results for a pair of NN Eu^{2+} ions in PbSe were obtained for angles $\phi=0$, 45°, and 90° between **H** and **r**. For each ϕ the separation $\Delta H=H_{n+1}-H_n$ depends on n, but this dependence is much weaker than that caused by the single-ion anisotropy. Due to the second term in Eq. (6) the average separation $(\Delta H)_{\rm av}$ is reduced by 6% for both $\phi=0$ and $\phi=45°$, and by 9% for $\phi=90°$. Since the first term in Eq. (6) increases ΔH by 6%, the net change of $(\Delta H)_{\rm av}$ due to the DD interaction is no more than 3% in all cases. If J is obtained from a fit of H_2 through H_7 to Eq. (5) then the net change due to the DD interaction is only 1% for all three ϕ's.

Although $(\Delta H)_{\rm av}$ is nearly independent of ϕ, the values of H_n vary by ~1 kOe as ϕ changes from zero to 90°. This variation is not negligible compared to the actual separation between adjacent MST's, $\Delta H\cong3.6$ kOe, and is important for the following reason. Each Eu ion in PbSe has 12 NN cation sites. In general, the vectors **r** for these NN sites make different angles ϕ with **H**. For example, when **H** is along [100], $\phi=45°$ for 8 NN's but for the other 4 NN's $\phi=90°$. In principle, the existence of several ϕ's and the fact that H_n depends on ϕ will cause a fine structure to appear in the MST's. When this fine structure is not resolved, which is the case in practice, it will make an additional contribution to the width δH of the MST's. Due to the extra width, the temperature requirement for resolving the MST's will be more stringent.

4. Combined single-ion and dipole-dipole anisotropies

The combined effect of the single-ion and DD anisotropies was calculated for several field directions. Examples of the results are the following. For $\mathbf{H}\|[100]$ there are two groups of NN's, with $\phi=45°$ or 90°. Compared to $(\Delta H)_J$, $(\Delta H)_{\rm av}$ is 9% higher for the first group and 7% higher for the second group. For $\mathbf{H}\|[110]$ there are three groups of NN's, with $\phi=0°$, 60°, and 90°. Compared to $(\Delta H)_J$ the changes in $(\Delta H)_{\rm av}$ are -3%, -4%, and -10%, respectively. All these changes in $(\Delta H)_{\rm av}$ are not very different from the sum of the changes caused by the two anisotropies separately.

III. EXPERIMENT

The three single crystals of $Pb_{1-x}Eu_xSe$ used in the experiments were grown by the Bridgman method. The Eu concentration x was obtained from the saturation magnetization at low temperatures, including a small correction for the lattice diamagnetic susceptibility $\chi_d=-3.6\times10^{-7}$ emu/g (Refs. 19 and 20). Assuming a saturation moment of $7.0\mu_B$ per Eu^{2+} ion, the results were $x=1.3$, 3.0, and 4.1 %. Similar values (1.2, 2.9, and 4.1 %) were derived from the Curie constants which were obtained from low-field susceptibility data. The susceptibility was measured with a superconducting quantum interference device (SQUID) magnetometer manufactured by Quantum Design Inc.

Magnetization measurements at low temperatures ($T<1$ K) were carried out with two systems. One system used a force magnetometer, a plastic dilution refrigerator, and a 55 kOe superconducting magnet.[10,21] The magnetic force was produced by a magnetic-field gradient, which was superimposed on the main field of the superconducting magnet. Both dc and ac gradients were used. In the case of a dc gradient the temperature was between 20 and 30 mK. With the ac gradient, a tiny amount of heat was generated by eddy cur-

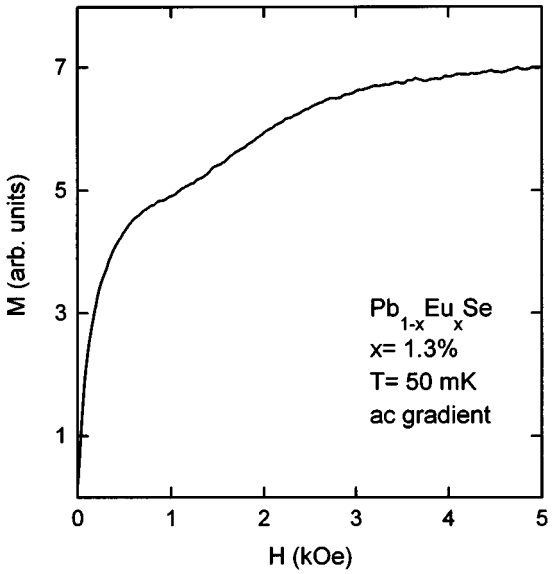

FIG. 5. Magnetization curve for $x=1.3\%$, measured at 50 mK. The magnetic field **H** is parallel to [100] within 5°. These data were obtained with an ac field gradient. To display the MST due to singles clearly, only data below 5 kOe are shown.

rents (there were a few small metallic components), and the temperature was near 50 mK. The second magnetometer system consisted of a vibrating sample magnetometer (VSM) operating in a 190-kOe Bitter magnet. Temperatures near 0.6 K were obtained by immersing the samples in pumped liquid ^{3}He.

IV. RESULTS AND DISCUSSION

A. MST due to isolated ions

The MST due to isolated Eu ions (singles) was observed in the sample with $x=1.3\%$. These data were taken in the dilution refrigerator. The sample was mounted with a (100) cleaved face perpendicular to **H**. The angle θ between **H** and the [100] direction was estimated to be less than 5°. Some of the results are shown in Fig. 5. They closely resemble the predicted behavior for $T=50$ mK [Fig. 1(b)]. The ratio between the magnetizations before and after the MST is approximately 5/7, as predicted.

The derivative dM/dH of the curve in Fig. 5 (not shown) exhibits a peak. After subtracting the monotonic background, the field at the peak gives the position of the MST as $H_c=1.76\pm0.2$ kOe. The large uncertainty is due to the fact that the peak is broad, with a flat top. The predicted value for H_c is 1.98 kOe. Considering the experimental uncertainty, and a possible small shift to lower H due to a finite θ, the agreement is quite reasonable.

B. Magnetization of pairs and open triplets at $T\leqslant 50$ mK

Examples of magnetization curves measured in the dilution refrigerator are shown in Figs. 6(a) and 6(b). These data are for $x=4.1$ and 3.0 %. Unlike the case of $x=1.3\%$, the direction of **H** was not controlled in these experiments. The curve for each of the two samples is the average of all traces obtained with a dc gradient. For $x=3.0\%$ similar data were also obtained with an ac gradient. Figures 6(a) and 6(b) show a rapid rise of M at low fields. This rise is attributed to the rapid alignment of the singles, but with some contribution from the OT's and CT's. The MST due to singles was not observed with these samples, probably because **H** was not aligned along one of the ⟨100⟩ directions.

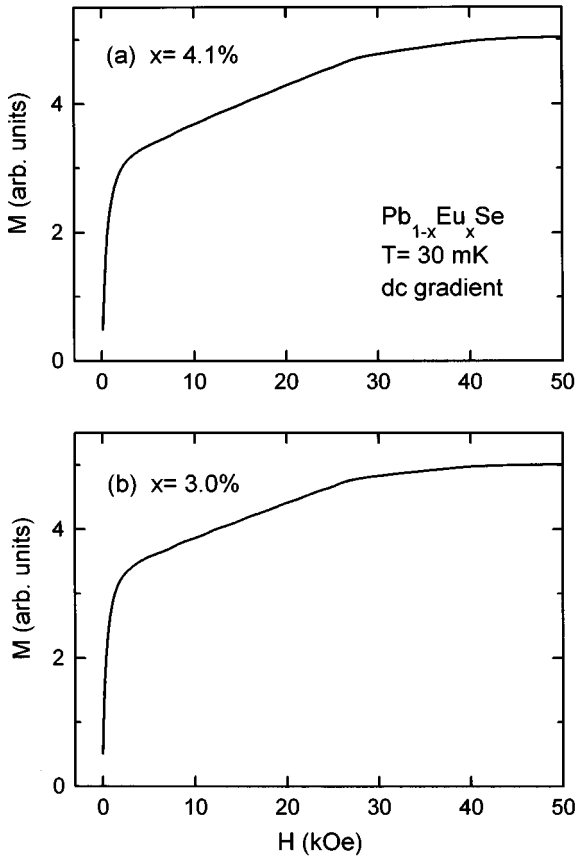

FIG. 6. Magnetization curves measured at 30 mK using a dc gradient. (a) Data for $x=4.1\%$. (b) Data for $x=3.0\%$.

Following the rapid rise at low fields, the magnetization in either Figs. 6(a) or 6(b) exhibits a ramp which is attributed to pairs. After this ramp ends, near 27 kOe, there is another ramp with a smaller slope. This second ramp is mainly due to OT's. (The ramp due to the OT's actually starts well below 27 kOe, but in that field range it is masked by the ramp from the pairs.) The ramp due to the OT's ends near 40 kOe.

When the vertical scale of Figs. 6(a) and 6(b) is expanded, the ramp due to the pairs exhibits well-resolved MST's. These MST's are also revealed by the derivative dM/dH, obtained by numerical differentiation of the magnetization curve after some data smoothing. The derivative curves are shown in Figs. 7(a) and 7(b). The last six MST's due to pairs ($n=2,3,\ldots,7$) are clearly visible for both samples. The first MST due to pairs ($n=1$) is obscured by the initial large drop in dM/dH, but in Fig. 7(b) it still manifests itself as a "shoulder" in the derivative curve. The peaks in dM/dH which correspond to MST's with $n=2$ and 3 seem to be more prominent than the peaks for higher n. Such a behavior is expected from the simulation in Fig. 4. When the ramp due to pairs ends, near 27 kOe, there is a drop in dM/dH. A smaller drop of dM/dH occurs when the ramp due to the OT's ends near 40 kOe.

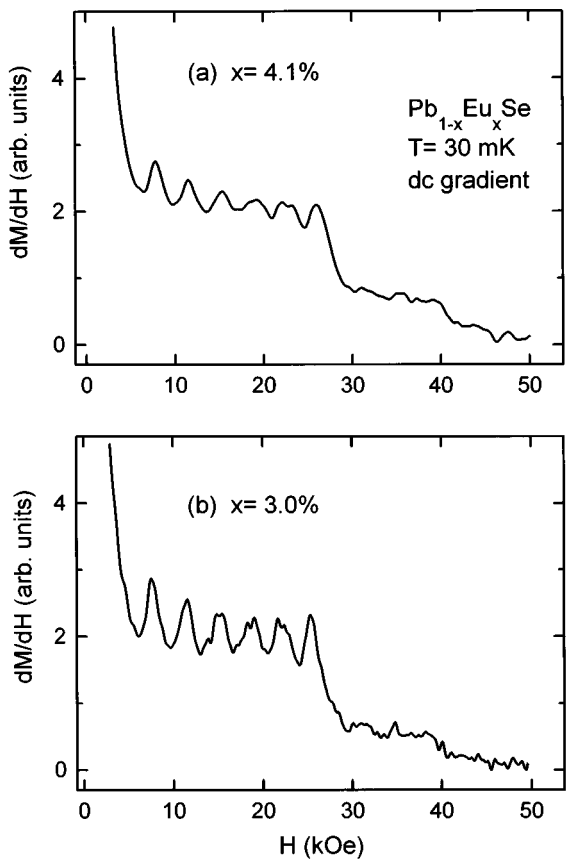

FIG. 7. The derivative dM/dH of the magnetization curves in Figs. 6(a) and 6(b).

Above 5 kOe the magnetization curve for $x=1.3\%$ (not shown) also exhibits a ramp due to pairs. This ramp is in fields above the MST due to singles. As in the other two samples the ramp due to pairs ends near 27 kOe, but for this lower x the MST's due to pairs can be resolved only after extensive data smoothing. The ramp due to the OT's is not seen clearly for $x=1.3\%$, presumably because the concentration of OT's is lower than in the other two samples.

C. The dominant AF exchange constant

The exchange constant J was obtained from the MST's due to pairs. The fields at the peaks of dM/dH [Figs. 7(a) and 7(b), and other similar results] were chosen as H_n. The fields H_2 through H_7 were fitted to Eq. (5), with Δ_n taken as a constant. With the known g value the only two parameters in this linear fit were J and Δ_n. All sets of H_n for $x=3.0$ and 4.1% were well fitted by Eq. (5), and they all gave very similar results, namely, $J/k_B=-0.24$ K and $\Delta_n/g\mu_B\cong 0.7$ kOe. The spread in the values of J was only 2%. However, in view of possible effects due to anisotropies (calculated in Sec. II C) our final result is $J/k_B=-0.24\pm 0.03$ K.

Only one AF exchange constant ($J/k_B=-0.24$ K) was observed in the present experiments. The following arguments indicate that it is the largest AF exchange constant. First, magnetization data at 0.6 K (discussed later) show no other MST's or ramps between 40 and 180 kOe. This means that there is no larger AF exchange constant, unless it is larger than 12 K in which case the MST's will occur at still higher fields. Second, a rough estimate of the dominant exchange constant can be obtained from the Curie-Weiss temperatures Θ (see, e.g., Ref. 9). This estimate depends on whether the NN or NNN exchange constant is the largest, but there is only a factor of 2 difference between the two choices. Values of Θ were obtained from low-field susceptibility data, performed on all three samples using a SQUID magnetometer. The results (e.g., $\Theta\cong -0.6$ K for $x=3.0\%$) showed that the dominant exchange constant is antiferromagnetic, and its magnitude is only a fraction of 1 K. Thus it cannot be higher than 12 K.

D. Identity of the dominant AF exchange constant

There are two likely possibilities for the identity of the dominant AF exchange constant, $J/k_B=-0.24\pm 0.03$ K. Either it is J_1 (for NN's) or it is J_2 (for NNN's). The method used to identify J is based on the fact that there are 12 NN sites but only 6 NNN sites in the fcc cation lattice. Assuming a random distribution of Eu ions over the cation sites (which is the key assumption), the calculated ramp due to NN pairs is substantially larger if J is J_1 than if it is J_2. The size of the calculated ramp due to OT's is also different. The identification of J is based on a comparison between the sizes of the observed ramps and those calculated by assuming that J is either J_1 or J_2.

The calculated magnetization curves were based on the model in Sec. II B, and they included singles, pairs, OT's, and CT's. The probabilities of finding these clusters were obtained from Behringer.[17] (His results are only for clusters with NN coupling, $J=J_1$, but they are given for several lattices. It is then useful to notice that the probabilities for clusters with NNN coupling only, $J=J_2$, when the lattice is fcc are the same as those for NN coupling when the lattice is simple cubic.) Only thermal broadening of the MST's was included in the simulations. However, since the MST's observed at 30 or 50 mK showed an additional broadening, a higher effective temperature, $T_{\rm eff}=100$ mK, was used in the simulations. The use of a higher temperature had no effect on the sizes of the calculated ramps, and therefore did not influence the identification of J.

To compare the shapes of the calculated magnetization curves with the measured curves, all curves were normalized so that they agreed at the highest field. Figures 8(a) and 8(b) show the comparison for $x=3.0\%$. The experimental curve in Fig. 8(a) is the average of all traces obtained with a dc gradient, while the very similar curve in Fig. 8(b) is the average for an ac gradient. In either case the J_1 model (i.e., the calculation with $J=J_1$) simulates the data much better than the J_2 model. The comparisons for the other two samples (not shown) also indicate that the J_1 model is much better. On this basis the dominant AF exchange constant J is identified as the NN exchange constant J_1.

The method of identifying J assumed that the Eu ions were randomly distributed. Some justification for this assumption is that the J_1 model with a random distribution gives fairly good fits for data on three samples with different x. It is unlikely that good agreement for three samples is accidental.

The conclusion that $J=J_1$ applies to $Pb_{1-x}Eu_xSe$ with $x\ll 1$. For pure EuSe, the accepted view is that J_1 is ferro-

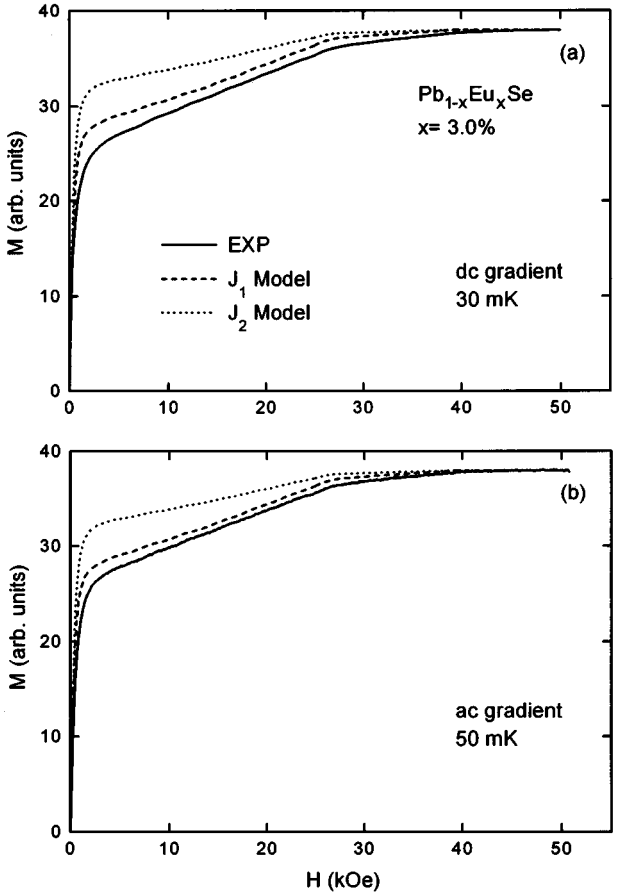

FIG. 8. Comparisons between theoretical simulations based on the J_1 and J_2 models and experimental data for $x=3.0\%$. (a) Comparison with data obtained at 30 mK using a dc gradient. (b) Comparison with data obtained at 50 mK using an ac gradient. To allow for nonthermal broadening, an effective temperature of 100 mK was used in the theoretical simulations (see text).

magnetic and J_2 is the largest AF exchange constant.[1] The present data do not agree with the accepted exchange constants for pure EuSe. Data analysis which included both a ferromagnetic J_1 and an antiferromagnetic J_2 was performed, using the probabilities which follow from a random distribution.[22] The results showed no significant improvement over the J_2 model, with J_2 only. The main reason why adding a ferromagnetic J_1 does not improve the fits significantly is that ferromagnetic clusters align rapidly at low H, so that they do not increase the sizes of the ramps at higher fields.

Since both EuSe and PbSe have the rocksalt structure, it is somewhat surprising that J_1 is ferromagnetic in EuSe but is AF for a small Eu concentration in PbSe. The difference in the sign of J_1 is presumed to be related to the very different electronic structures of EuSe and PbSe. The mechanisms responsible for J_1 and J_2 in EuSe are well known,[1,2] but this is not the case for Eu in PbSe. Indeed, even the location of the $4f^7$ levels of the Eu^{2+} ion with respect to the PbSe band structure has not been established.[6] In EuSe the dominant mechanism responsible for the ferromagnetic J_1 involves the two Eu^{2+} cations but not the neighboring anion.[1,2] In contrast, it has been suggested by Górska *et al.*[6] that in rare-

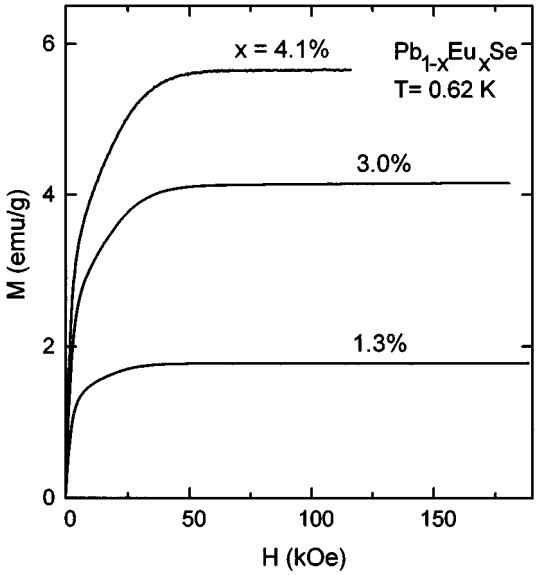

FIG. 9. Magnetization curves at 0.62 K for all three samples. These experimental results include the (small) correction for the diamagnetism of the lattice.

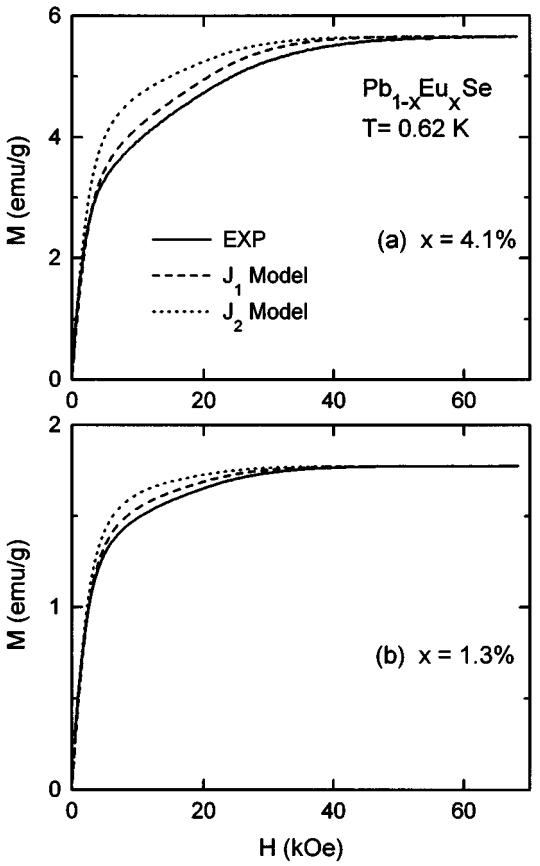

FIG. 10. Comparisons between two of the experimental curves in Fig. 9 and theoretical simulations based on the J_1 and J_2 models. (a) Comparison for $x=4.1\%$. (b) Comparison for $x=1.3\%$.

earth-doped IV–VI DMS, a 90° superexchange via the anion may lead to a J_1 which is AF. A calculation, or even a theoretical estimate, of J_1 for Eu^{2+} ions in PbSe is not available at present to our knowledge.

Figures 8(a) and 8(b) (and similar results for the other samples) indicate that while the J_1 model is clearly superior to the J_2 model, it still fails to agree with the data perfectly. The remaining deviations are attributed to the simplicity of the model: no anisotropy, only one J, and only clusters with less than 4 spins. It is possible to improve on the J_1 model. For example, the experimental results for H_n show that these fields are shifted upward by about 0.7 kOe relative to the J_1 model, i.e., Eq. (5) rather than Eq. (1) applies. An upward shift by 0.7 kOe of the calculated ramps in Figs. 8(a) and 8(b) will improve the agreement with the data.

E. Magnetization curves at 0.6 K

The magnetization curves at 0.62 K for all the samples are shown in Fig. 9. These data have been corrected for the diamagnetic susceptibility of the lattice. The general shape of all three curves is the same: a fast rise of M at low H, followed by a rounded ramp, followed by full saturation at $H>50$ kOe.

Theoretical simulations of the magnetization curves in Fig. 9 were performed using the J_1 and J_2 models. The actual temperature was used in these simulations because at 0.62 K thermal broadening of the ramps is expected to dominate all other sources of broadening. (The extra broadening observed at $T\leqslant 50$ mK was equivalent to only 60 mK approximately.) The simulations for $x=4.1$ and 1.3% are compared with the data in Figs. 10(a) and 10(b). It is clear that the J_1 model gives a much better account for the experimental data. The simulations for the sample with $x=3.0\%$ (not shown) lead to the same conclusion. These results confirm that the dominant AF exchange constant is J_1.

V. CONCLUSIONS

A magnetization step arising from isolated Eu^{2+} ions was observed at 1.76 ± 0.2 kOe, which is close to the value 1.98 kOe expected from EPR data. The relatively low field at which this MST occurs is consistent with the expected low anisotropy for an S-state ion.

Magnetization ramps due to pairs and OT's were observed. At 30 and 50 mK, the ramp due to pairs consisted of well-resolved MST's. These MST's gave the value $J/k_B=-0.24\pm 0.03$ K for the dominant AF exchange constant. Such a small J confirms early indications[5,6] that exchange interactions in IV–VI DMS are much weaker than in the traditional II–VI DMS. Comparisons of the magnetization curves with theoretical simulations identify J as J_1, in contrast to pure EuSe for which the dominant AF exchange constant is J_2.

The availability of a magnetometer operating in a dilution refrigerator was crucial for the success of the present experiments. With such a magnetometer, weak exchange interactions between magnetic ions, and small anisotropies for isolated ions, can be measured by the MST method.

ACKNOWLEDGMENTS

This work was supported by CNPq, FAPESP, and FINEP (Brazilian agencies), by NSF Grants No. DMR-9219727 and No. INT-9216424, by CNRS (France), and by the Polish Committee for Scientific Research. The Francis Bitter National Magnet Laboratory is supported by NSF.

[1] A. Mauger and C. Godart, Phys. Rep. **141**, 51 (1986).
[2] P. Wachter, in *Handbook on the Physics and Chemistry of Rare Earths*, edited by K. A. Gschneidner, Jr. and L. Eyring (North-Holland, Amsterdam, 1979), Vol. I, p. 507 ff.
[3] E. L. Nagaev, *Physics of Magnetic Semiconductors* (Mir, Moscow, 1983).
[4] S. Methfessel and D. Mattis, in *Handbuch der Physik*, edited by S. Flügge (Springer, Berlin, 1968), Vol. XVIII/1, p. 389 ff.
[5] G. Bauer and H. Pascher, in *Semimagnetic Semiconductors and Diluted Magnetic Semiconductors*, edited by M. Averous and M. Balkanski (Plenum, New York, 1991), p. 209 ff.
[6] M. Górska, J. R. Anderson, G. Kido, and Z. Golacki, Solid State Commun. **75**, 363 (1990); M. Górska, J. R. Anderson, G. Kido, S. M. Green, and Z. Golacki, Phys. Rev. B **45**, 11 702 (1992).
[7] Y. Shapira, J. Appl. Phys. **67**, 5090 (1990).
[8] T. Q. Vu, V. Bindilatti, Y. Shapira, E. J. McNiff, Jr., C. C. Agosta, J. Papp, R. Kershaw, K. Dwight, and A. Wold, Phys. Rev. B **46**, 11 617 (1992).
[9] Y. Shapira, in *Semimagnetic Semiconductors and Diluted Magnetic Semiconductors*, edited by M. Averous and M. Balkanski (Plenum, New York, 1991), p. 121 ff; Y. Shapira, Acta Phys. Pol. **87**, 107 (1995).
[10] V. Bindilatti, A. N. Anisimov, N. F. Oliveira, Jr., Y. Shapira, M. Goiran, F. Yang, S. Isber, M. Averous, and M. Demianiuk, Phys. Rev. B **50**, 16 464 (1994); S. Isber, M. Averous, Y. Shapira, V. Bindilatti, A. N. Anisimov, N. F. Oliveira, Jr., V. M. Orera, and M. Demianiuk, *ibid.* **51**, 15 211 (1995).
[11] A. Abragam and B. Bleaney, *Electron Paramagnetic Resonance of Transition Ions* (Dover, New York, 1986), Secs. 3.4 and 5.9.
[12] S. Isber, S. Charar, C. Fau, V. Mathet, M. Averous, and Z. Golacki, Phys. Rev. B **52**, 1678 (1995).
[13] See, e.g., M. Kreitman, F. Milford, R. Kenan, and J. G. Daunt, Phys. Rev. **144**, 367 (1966).
[14] G. Bastard and C. Lewinger, J. Phys. C **13**, 1469 (1980).
[15] A. Bruno, J. P. Lascaray, M. Averous, J. M. Broto, J. C. Ousset, and J. F. Dumas, Phys. Rev. B **35**, 2068 (1987).
[16] X. Wang, D. Heiman, S. Foner, and P. Becla, Phys. Rev. B **41**, 1135 (1990).
[17] R. E. Behringer, J. Chem. Phys. **26**, 1504 (1957).
[18] B. E. Larson, K. C. Hass, and R. L. Aggarwal, Phys. Rev. B **33**, 1789 (1986).
[19] T. R. McGuire, B. E. Argyle, M. W. Shofer, and J. S. Smart, Appl. Phys. Lett. **1**, 17 (1962).
[20] J. R. Anderson, G. Kido, Y. Nishina, M. Gorska, L. Kowalczyk, and Z. Golacki, Phys. Rev. B **41**, 1014 (1990).
[21] V. Bindilatti and N. F. Oliveira, Jr., Physica B **194-196**, 63 (1994).
[22] M. M. Kreitman and D. L. Barnett, J. Chem. Phys. **43**, 364 (1965).